

Methods for differential network estimation: an empirical comparison

Anna Plaksienko^{1*}, Magne Thoresen¹, and Vera Djordjilović²

¹Oslo Centre for Biostatistics and Epidemiology, Department of Biostatistics, University of Oslo, Oslo, Norway

²Department of Economics, Ca' Foscari University of Venice, Venice, Italy

**email: annapla@uio.no*

December 2024

Abstract

We provide a review and a comparison of methods for differential network estimation in Gaussian graphical models with focus on structure learning. We consider the case of two datasets from distributions associated with two graphical models. In our simulations, we use five different methods to estimate differential networks. We vary graph structure and sparsity to explore their influence on performance in terms of power and false discovery rate. We demonstrate empirically that presence of hubs proves to be a challenge for all the methods, as well as increased density. We suggest local and global properties that are associated with this challenge. Direct estimation with lasso penalized D-trace loss is shown to perform the best across all combinations of network structure and sparsity.

Keywords: high-dimensional inference, differential networks, Gaussian graphical models, gene networks

1 Introduction

Nowadays, networks are used in many different areas of science in various forms, capturing different types of interactions between variables. With the rise of situations when datasets come from similar yet distinct conditions, it becomes more relevant to estimate the differences between those conditions, specifically in terms of networks. One example can be a molecular network of a healthy population compared to cancer patients: many genes are unrelated to the disease, so their connections would be identical in both groups. It might be more relevant to estimate the differential network, i.e., only the connections that are different between conditions. In this article, we highlight possible challenges in such differential network estimation. To the best of our knowledge, such issues were not previously discussed in the literature specifically for differential graph estimation. Therefore, we hope this manuscript may be helpful to others pursuing this field.

We refer the reader to (Shojaie, 2021) for the broad review of differential network estimation. Here, we define a narrower setting and perform a comparison of methods there.

Broadly, a network is a collection of vertices corresponding to some variables and edges, signifying some interaction between these variables that may be defined in various ways. In our work, we focus on graphical models – networks where edges signify conditional dependence, i.e., direct, unmediated connections between

variables (see the next section for the formal definition and (Lauritzen, 1996) for in-depth details). Although networks defined through marginal associations are relevant and of interest in many applications, we do not discuss them here.

Within graphical models, we focus specifically on undirected ones. Firstly, directed graphical models are more challenging to estimate (Zheng et al., 2018) and additional constraints are required in order to find a unique solution (Giraud, 2015). Secondly, in many cases, it is of interest to focus only on the presence of a connection, not necessarily its direction.

In the class of undirected graphical models, we consider those associated with the Gaussian distribution. As in many other situations, this particular distribution has many unique theoretical properties that make its use beneficial. In the case of graphical models, it is the fact that Gaussian graph structure can be estimated through a precision (inverse covariance) matrix.

In addition, we assume that data comes in the form of two datasets from similar but different conditions. It can be measurements of the same variables processed on different equipment or in different locations, the same system under various stimulating conditions, different subtypes of diseases, possibly different time points. We assume that there are edges (connections) that coincide in the graphical models from two conditions, but that there are also differences and we aim to capture those.

In this manuscript, we apply a frequentist approach and do not discuss Bayesian methods, although many exist (see, for example (Zhao et al., 2023)). This choice was made mainly for better comparability of the methods.

We include methods both with and without error control in the comparison, in order to more comprehensively assess various approaches. However, we would like to emphasize the importance of error control, especially in biological settings.

Most standard methods for estimation of Gaussian graphical models (like the graphical lasso) implicitly assume a uniformly random network, and hence, so do methods for differential network estimation. However, there is clear evidence that this might not be a realistic enough model for biological networks. Thus, it becomes important to investigate to what extent these methods are able to handle other structures as well.

The aim of the article is twofold. First, we will perform an evaluation and a comparison of available methods for differential network estimation through a simulation study. Our focus is on structure learning, so we measure performance by power and false discovery rate related to edge detection. Next, we will investigate the influence of graph structure on methods performance through the same simulation study.

We will start with the various definitions of a differential network. We will then demonstrate the variability of the results of the existing methods for the differential network estimation with a real data example, thus emphasizing the importance of error control. Next, we will describe the estimation methods and compare them in the simulation study, highlighting their advantages and downsides. We will discuss how different graph structures influence the performance of those methods as a class and each of them individually. In the end, we will mention possible directions for future work.

Throughout the paper, matrices are denoted by bold capital letters \mathbf{M} . Their scalar entries are denoted with non-bold letters with two lower case indices, e.g. M_{ij} . Bold lower case letters denote vectors, i.e. $\boldsymbol{\mu}$. Bold italic upper case letters denote random vectors, e.g. \mathbf{X} , and non-bold italic upper case letters with one lower index denote random variables, e.g. V_i . Non-bold lower case letters with or without a lower index denote scalars, i.e. λ_2 .

1.1 What is a differential network?

First, we would like to highlight that multiple definitions of differential networks exist. Let us first define a Gaussian graphical model. We start with a p -variate zero mean Gaussian distribution of variables $\mathbf{X} = (X_1, \dots, X_p)^T$ with a covariance matrix Σ . Note that we assume that the mean vector is zero without loss of generality, since the covariance structure, modeled by the graphical model, is structurally independent from the mean vector. We can represent this distribution $\mathcal{N}(0, \Sigma)$ in terms of the graph $G = (V, E)$, where $V = \{1, \dots, p\}$ is the set of vertices and $E \subseteq V \times V$ is the set of edges. Each vertex i corresponds to a random variable X_i , and the absence of an edge between vertices i and j implies conditional independence of the corresponding variables, i.e., $(i, j) \notin E \Leftrightarrow X_i \perp\!\!\!\perp X_j \mid \mathbf{X}_{\{l, l \neq i, j\}}$, where \mathbf{X}_U is a subvector of \mathbf{X} for any $U \subset V$. In the Gaussian setting, the support of the precision matrix $\Omega = \Sigma^{-1}$ encodes the graph structure. Let \mathbf{A} denote the adjacency matrix of graph G , then $A_{ij} = 0$ if and only if $\Omega_{ij} = 0$.

Now let us consider two distributions instead of one, $\mathcal{N}(0, \Sigma^{(1)})$ and $\mathcal{N}(0, \Sigma^{(2)})$. They can describe two conditions, such as subtypes of a disease or data collected on different equipment or in different laboratories. In this case, it is of interest to investigate the differences between the two distributions. We can do so in terms of graphs again, as supports of precision matrices $\Omega^{(1)}$ and $\Omega^{(2)}$ encode graphs' $G^{(1)}$ and $G^{(2)}$ adjacency matrices $\mathbf{A}^{(1)}$ and $\mathbf{A}^{(2)}$. However, how do we define a differential network?

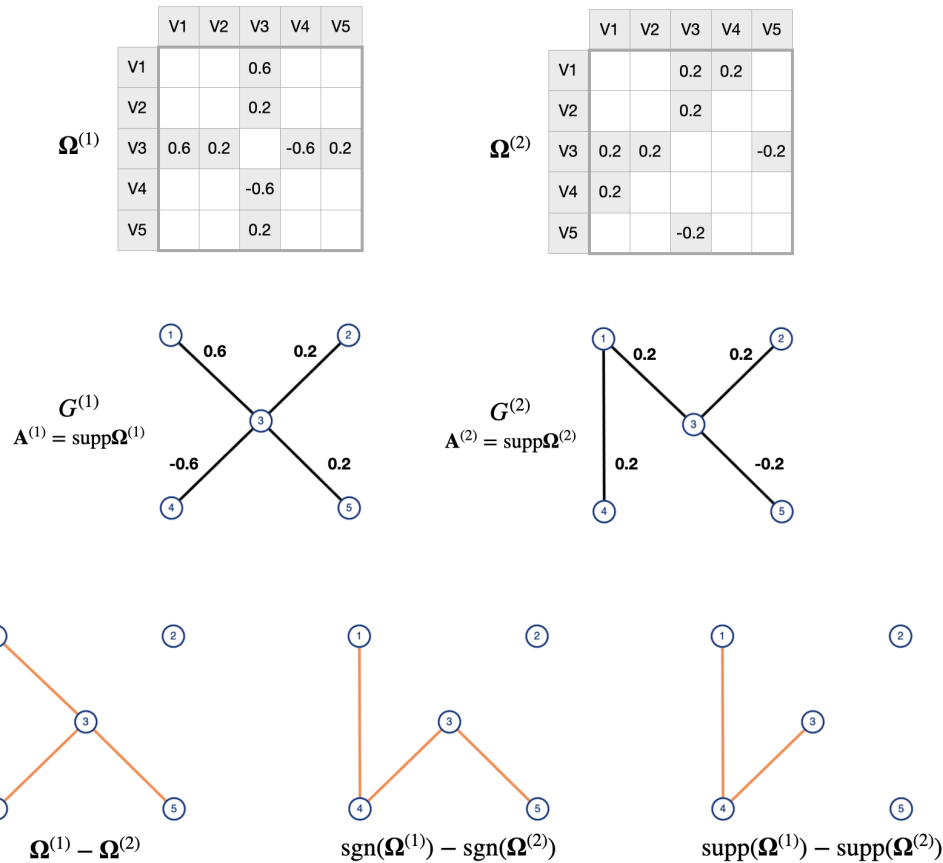


Figure 1: Illustration of different definitions of differential networks. Top: precision matrices for two populations (blank squares represent zero entries). Center: graphs of the two Gaussian graphical models. Bottom: differential networks based on differences in values (left), differences in sign (center) and differences in support (right).

The difference between two networks can be assessed in a number of ways. We report the three most prevalent definitions of a differential network within the Gaussian graphical models context. Let $G^{diff} = (V, E^{diff})$ denote a differential graph. Its edge set E^{diff} can be defined as follows.

Definition 1 (Difference in value)

$$E^{diff} = \left\{ (i, j) : \Omega_{ij}^{(1)} \neq \Omega_{ij}^{(2)} \right\}. \tag{1}$$

Definition 1 identifies as different, node pairs for which the corresponding elements of the two precision matrices are different. It captures quantitative differences between the two networks and is the most prevalent definition used in the literature. A difference in value may reflect either a difference in structure or a difference in the strength of a relationship between the associated variables. As an alternative, Definition 2 is capturing qualitative differences. It identifies as different, node pairs for which the sign of the corresponding elements of the two precision matrices is different.

Definition 2 (Difference in sign)

$$E^{diff} = \left\{ (i, j) : \text{sgn} \left(\Omega_{ij}^{(1)} \right) \neq \text{sgn} \left(\Omega_{ij}^{(2)} \right) \right\}, \tag{2}$$

where $\text{sgn}(x) = 1$ for $x > 0$, $\text{sgn}(x) = -1$ for $x < 0$, and $\text{sgn}(x) = 0$ otherwise.

Definition 2 is thus capturing differences in structure and a subset of differences in values: those corresponding to a sign switch. Finally, Definition 3 captures solely differences in structure.

Definition 3 (Difference in support)

$$E^{diff} = \left\{ (i, j) : A_{ij}^{(1)} \neq A_{ij}^{(2)} \right\}. \tag{3}$$

Figure 1 illustrates the three definitions of a differential network. The choice of which definition to use in practical applications should be guided by subject matter considerations. Most methods reviewed here use Definition 1, with the exception of differential connectivity analysis (DCA), that uses Definition 3. Our simulation studies are designed so that differential networks according to the three definitions coincide.

1.2 TCGA breast cancer dataset analysis

Before describing the various methods, we would like to present a real data example to demonstrate how vastly the results vary. In our opinion, this variability highlights the challenge in differential network estimation and emphasizes the need for reliable methods with error control.

In (Koboldt et al., 2012), the authors collected 526 samples of patients with breast cancer of four molecular subtypes: luminal A, luminal B, basal-like, and HER2-enriched cancers. The original microarray gene expression dataset has 17 327 genes. For this analysis, we use a pre-processed sub-dataset available in the `DiffNetFDR` R package (Zhang et al., 2019). It consists of two datasets, luminal A subtype with $n_1 = 231$ samples and basal-like subtype with $n_2 = 95$ samples, and $p = 139$ genes from the hsa05224 KEGG (Kanehisa and Goto, 2000) breast cancer pathway.

To identify gene connections that differ between luminal A and basal-like subtypes of breast cancer, we used five different differential network estimation methods. We will describe each method in detail in the following section. Here, however, we would like to focus on the variability of the methods’ results.

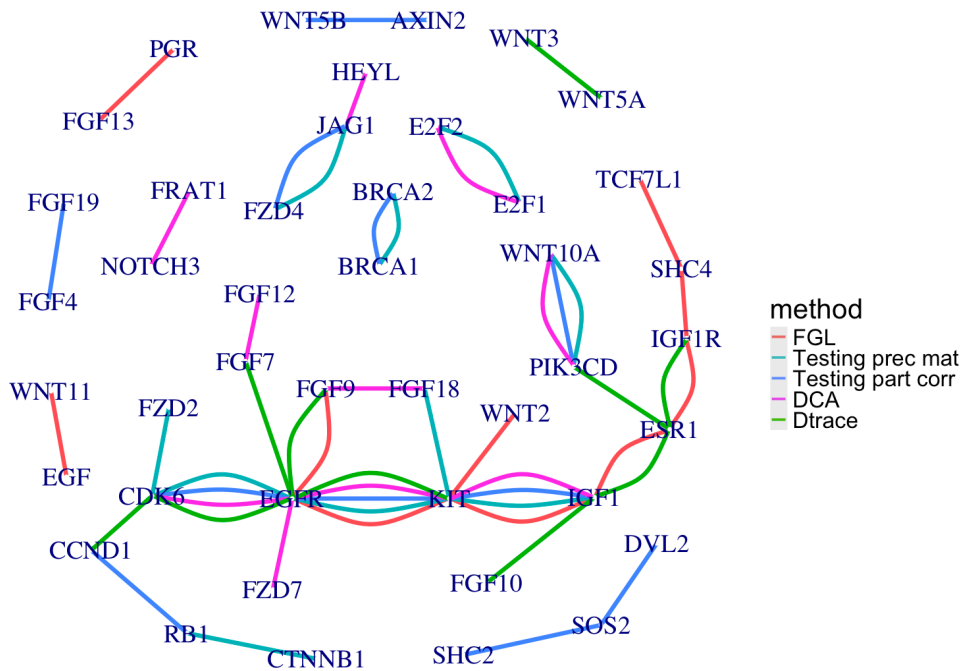


Figure 2: Figure demonstrates the variability of results, produced with different methods. Multiplicity of an edge denotes how many methods have identified it and the color corresponds to a method.

To assess the results of the methods based on the different approaches and with various tuning parameters, we have decided to choose the network size as the common denominator. Although it is not a universal practice, aiming for a small network size in the estimation is not uncommon to improve interpretability. Therefore, in this example, we compare five 10-edge networks produced by five different methods. The parameters we used to obtain these estimates are provided in Appendix 4.

Out of the original 139 vertices (genes), 96 are estimated to be isolated by all the methods. The size of the union of all five 10-edge networks is 33 edges. Interestingly, only one edge was identified by all five methods, and only two edges were identified by four methods. Most of the edges were estimated by one method only (see Table 1 and Figure 2). This indicates the difficulty of differential network estimation, and we use this example to highlight it and to motivate our further investigation.

Table 1: A frequency table showing the number of methods, m , whose estimated differential networks have l common edges, i.e. no edge was present in all five estimated differential networks, three edges were present in four networks, one edge was estimated by three methods. . .

Number of methods m	5	4	3	2	1
Number of edges l	1	2	1	6	23

The only edge that was estimated by all five methods is the EGFR-KIT edge. The authors of (Nalwoga et al., 2008) and (Kanapathy Pillai et al., 2012) report that expression of these genes is associated with basal-like breast cancer subtype which may suggest that this edge is a true differential edge (i.e. present in basal-like type but not in luminal A). The two edges that were estimated by 4 out of 5 methods are IGF1-KIT and EGFR-CDK6. We were not able to find evidence in the literature that these connections

may be differential between luminal A and basal-like breast cancer subtypes.

2 Methods

In this section, we present methods for estimating a differential network. We discuss only methods that provide an estimate of a differential network, that is, we do not consider methods that perform global testing of equality of two Gaussian distributions without estimating the differential structure itself.

Methods for estimating a differential network can be divided into three categories, as follows.

Joint estimation of multiple Gaussian graphical models. These methods were designed to estimate multiple related Gaussian graphical models that are expected to have a partially common structure while exhibiting some differences. The output consists of the two condition specific networks, and it is up to the user to, given the results, construct a differential network. We consider one method in this category: joint graphical lasso with fused penalty or, for short, the fused graphical lasso (FGL) (Danaher et al., 2014).

Testing-based methods. These methods obtain an estimate of a differential network by testing equality of the entries of a partial correlation matrix (Liu, 2017), a precision matrix (Xia et al., 2015), or an adjacency matrix (Zhao and Shojaie, 2022) in two conditions.

Direct estimation. These methods estimate a differential network directly, without estimating condition specific networks (Zhao et al., 2014; Yuan et al., 2017). We will discuss one such method, with lasso penalized D-trace loss (Yuan et al., 2017).

In our simulation study, we consider representatives of each category. Our choice of specific methods was mainly guided by the software availability: we included only methods that have available implementation in R. An overview of the considered methods is given in Table 2 with a brief description of each.

Table 2: Summary of methods for estimation of differential networks.

Name	Reference	Type	Estimand	Error control	R package	Tun. param.
FGL	(Danaher et al., 2014)	Joint estim.	$\Omega^{(1)}, \Omega^{(2)}$	No	JGL	λ_1, λ_2
pcor	(Liu, 2017)	Testing	$E^{diff} = \{(i, j) : \rho_{ij}^{(1)} \neq \rho_{ij}^{(2)}\}$	Asymp. FDR	DiffNetFDR	No
pmat	(Xia et al., 2015)	Testing	$E^{diff} = \{(i, j) : \Omega_{ij}^{(1)} \neq \Omega_{ij}^{(2)}\}$	Asymp. FDR	DiffNetFDR	No
DCA	(Zhao and Shojaie, 2022)	Testing	$E^{diff} = \{(i, j) : A_{ij}^{(1)} \neq A_{ij}^{(2)}\}$	Asymp. FDR	DCA	No
D-trace	(Yuan et al., 2017)	Direct estim.	$\Omega^{(1)} - \Omega^{(2)}$	No	DiffGraph	λ

We use the following notation. Suppose we are given two datasets $\mathbf{X}^{(k)}$, $k = 1, 2$, each with n_k independent, identically distributed observations from $\mathcal{N}(0, \Sigma^{(k)})$. We denote empirical covariance matrices as $\mathbf{S}^{(k)} = \frac{1}{n_k} (\mathbf{X}^{(k)})^\top \mathbf{X}^{(k)}$. We note that some of the presented methods consider $K > 2$ datasets but for simplicity and comparability we will consider only the case of $K = 2$.

2.1 Fused graphical lasso (FGL)

Fused graphical lasso (Danaher et al., 2014) is a likelihood-based method for joint estimation of multiple graphical models from datasets with observations belonging to distinct classes. Although it is not the first method in this class – an earlier example can be (Guo et al., 2011) – it is currently one of the most mentioned

in the literature. The aim is to estimate two graphical models under the assumption that both networks are sparse and at the same time enforcing some similarity between the networks. In the high dimensional case of p bigger than n_k , $k = 1, 2$, the authors suggest to maximize the following penalized log-likelihood function:

$$\sum_{k=1}^2 n_k \left\{ \log(\det \boldsymbol{\Omega}^{(k)}) - \text{tr} \left(\mathbf{S}^{(k)} \boldsymbol{\Omega}^{(k)} \right) \right\} - \lambda_1 \sum_{k=1}^2 \sum_{i \neq j} |\Omega_{ij}^{(k)}| - \lambda_2 \sum_{i,j} |\Omega_{ij}^{(1)} - \Omega_{ij}^{(2)}|, \quad (4)$$

where λ_1 and λ_2 are non-negative tuning parameters. The penalty term corresponding to λ_1 drives the sparsity of the estimated precision matrices, while the term corresponding to λ_2 encourages equality of entries across classes. The solution of (4) is called the fused graphical lasso (FGL).

In the paper, the authors suggest to construct a differential network according to the difference in the entries of the estimated precision matrices, i.e. when $\hat{\Omega}_{ij}^{(1)} \neq \hat{\Omega}_{ij}^{(2)}$ (Definition 1). However, we will follow the approach from their simulation code and account for possible computational errors, defining an edge (i, j) as differential if $|\hat{\Omega}_{ij}^{(1)} - \hat{\Omega}_{ij}^{(2)}| > 10^{-3}$.

We use the authors' R package JGL available on CRAN.

2.2 Testing equality of partial correlations

The authors of (Liu, 2017) define a differential network through partial correlations. A partial correlation coefficient of X_i and X_j given $X_{l \neq i, j}$ can be expressed through precision matrix entries as $\rho_{ij} = -\Omega_{ij} / \sqrt{\Omega_{ii} \Omega_{jj}}$. For two conditions, their differential graph is defined similarly to Definition 1 as

$$E^{diff} = \{(i, j) : \rho_{ij}^{(1)} \neq \rho_{ij}^{(2)}\}.$$

The differential graph is estimated through a multiple testing procedure testing a collection of null hypotheses $\{H_{ij} : \rho_{ij}^{(1)} = \rho_{ij}^{(2)}, 1 \leq i < j \leq p\}$. The authors prove that the proposed procedure provides asymptotic false discovery rate control, and further recover an approximation of the set of common edges, again with false discovery rate control. We refer interested readers to the original article for further details.

In our simulation study, we used the implementation from the `DiffNetFDR` R package available on Github, which was not developed by the authors of the method, see software article (Zhang et al., 2019) for further details.

2.3 Testing equality of the entries of precision matrices

In (Xia et al., 2015), a differential network is defined according to Definition 1, as the difference between entries of precision matrices. The authors first perform a test of a global null hypothesis $H_0 : \boldsymbol{\Omega}^{(1)} = \boldsymbol{\Omega}^{(2)}$ and if it is rejected, investigate the structure of the differential network with a multiple testing procedure for a collection of null hypotheses $\{H_{ij} : \Omega_{ij}^{(1)} = \Omega_{ij}^{(2)}, 1 \leq i < j \leq p\}$. To perform the test of H_{ij} , the authors estimate $\boldsymbol{\Omega}^{(k)}$ by its relation with the coefficients of a set of node-wise linear regression models for $\mathbf{X}^{(k)}$. The test statistics are then obtained as covariances between the residuals of the fitted models.

There is a Matlab implementation by the method's authors. In our simulation study, we used the implementation from the `DiffNetFDR` R package available on Github (Zhang et al., 2019).

For other methods testing the equality of precision matrices entries, we refer the reader to (He et al., 2019), (Belilovsky et al., 2016) (estimates individual precision matrices with debiased lasso) or (Zhang et al., 2023) (uses a symmetrized data aggregation strategy).

2.4 Differential connectivity analysis (DCA)

The authors of (Zhao and Shojaie, 2022) define a differential network through differences in structure of individual networks, i.e., differences in supports of precision matrices (Definition 3). Therefore, they suggest testing qualitative differences, rather than quantitative differences like the methods described above. The method is based on testing a collection of null hypotheses

$$\left\{ H_i : \text{ne}_i^{(1)} = \text{ne}_i^{(2)}, 1 \leq i \leq p \right\},$$

where $\text{ne}_i^{(k)}$ is the set of neighbours of node i in $G^{(k)}$, i.e. $\text{ne}_i^{(k)} = \{j : (i, j) \in E^{(k)}\}$. To test this collection, a two-step procedure is proposed. First, two condition specific networks are estimated separately by any procedure that satisfies certain coverage conditions. In their manuscript, the authors use regression-based neighbourhood estimation (Meinshausen and Bühlmann, 2006). For each node, an estimate of a set of common neighbors $\widehat{\text{ne}}_i^0$ is obtained as an intersection of the two condition specific neighborhoods: $\widehat{\text{ne}}_i^0 = \widehat{\text{ne}}_i^{(1)} \cap \widehat{\text{ne}}_i^{(2)}$. In the second step, it is tested that there is no node j , such that $j \notin \widehat{\text{ne}}_i^0$ and $(i, j) \in \widehat{\text{ne}}_i^{(1)} \cup \widehat{\text{ne}}_i^{(2)}$, i.e. there is no j such that the edge (i, j) is not a common edge, but it is present in one of the two estimated condition specific networks.

There is a challenge of "double-dipping" – the same data is used both to formulate and to test the hypotheses. To address this issue, the authors adopt a data splitting approach. In their simulation study, they compare it with the naïve approach, which treats hypotheses as data-independent. Not surprisingly, the naive approach was superior in statistical power, but, somewhat surprisingly, also in controlling false discovery rate. This was explained by the fact that the crucial assumption for controlling false discovery rate asymptotically is that the true common neighbourhood of each node is covered by its estimator with probability tending to 1. This event is less likely to happen with smaller sample sizes that arise with sample splitting.

In our simulation study, we used the authors' R package `DCA` available on Github (not to be confused with the package of the same name on CRAN).

2.5 Direct estimation with lasso penalized D-trace loss (Dtrace)

Here, we introduce an approach originally proposed in (Zhao et al., 2014) and improved in (Yuan et al., 2017). If $\mathbf{S}^{(k)}$, $k = 1, 2$, denotes a sample covariance matrix, it is suggested to estimate $\mathbf{\Delta} = \mathbf{\Omega}^{(1)} - \mathbf{\Omega}^{(2)}$ directly by minimizing a convex loss function

$$L_D(\mathbf{\Delta}, \mathbf{S}^{(1)}, \mathbf{S}^{(2)}) + \lambda \|\mathbf{\Delta}\|_1,$$

where

$$\begin{aligned} L_D(\mathbf{\Delta}, \mathbf{S}^{(1)}, \mathbf{S}^{(2)}) &= \frac{1}{4} \left(\langle \mathbf{S}^{(1)} \mathbf{\Delta}, \mathbf{\Delta} \mathbf{S}^{(2)} \rangle + \langle \mathbf{S}^{(2)} \mathbf{\Delta}, \mathbf{\Delta} \mathbf{S}^{(1)} \rangle \right) \\ &\quad + \langle \mathbf{\Delta}, \mathbf{S}^{(1)} - \mathbf{S}^{(2)} \rangle. \end{aligned}$$

is a D-trace loss function, with $\langle A, B \rangle = \text{tr}(AB^\top)$, $\|A\|_1 = \sum_{i,j=1}^p |a_{ij}|$, and $\lambda > 0$ a tuning parameter.

Similarly to the fused graphical lasso, the authors suggest to use alternating direction method of multipliers to solve the problem.

We used the implementation of the method from the `DiffGraph` R package available on GitHub (not developed by the authors of the method, see software article (Zhang et al., 2018)).

3 Simulation study

3.1 Study set-up

In this section, we introduce our simulation study set-up. To assess the methods’ performance, we decided to vary the structure of the differential network, the sparsity of the graphs, and the number of samples in the data. We elaborate on parameter configurations below.

3.1.1 Graph generation

In this study, we would like to investigate to what extent the structure of the differential network influences the methods’ performance. It is well-known that presence of hubs (vertices with much higher degrees than the rest of the nodes in the graph) poses a challenge in estimation of graphical models (Tan et al., 2014) but, to the best of our knowledge, there are no studies on its effect in differential network estimation. However, in biological networks, hubs are likely to be present and efficient estimation of graphs with hubs is of utmost importance.

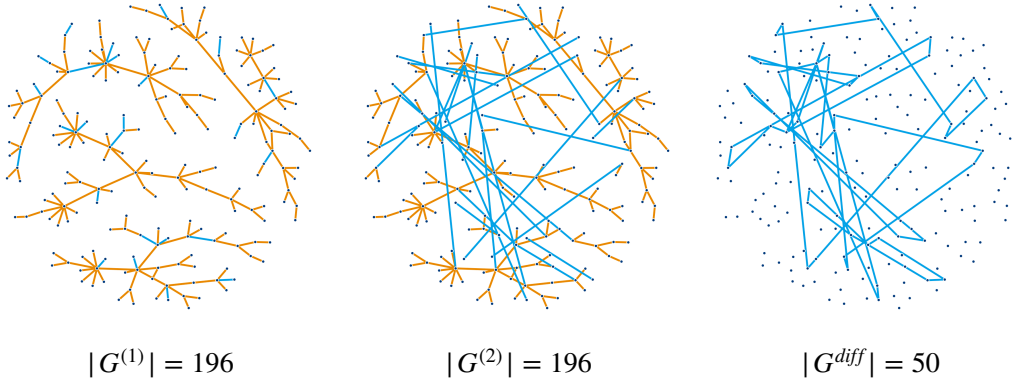
We consider three different structures of G^{diff} (see Figure 3):

1. **Random graph:** Start with a network $G^{(1)}$ that consists of several disconnected scale-free networks, i.e. its adjacency matrix is block-diagonal. Then, apply an iterative rewiring procedure. It randomly chooses pairs of edges (a, b) and (c, d) and switches them to obtain (a, c) and (b, d) edges. This produces a graph $G^{(2)}$ with the same size and degree distribution. The differential network G^{diff} has no prominent structure. This set-up acts as a baseline where standard methods are assumed to work well.
2. **Scale-free graph:** Start with the same network $G^{(1)}$ consisting of several disconnected scale-free networks. Remove some blocks (the number depends on what sparsity we want to achieve) and obtain $G^{(2)}$. The differential network G^{diff} consists of one or several disconnected scale-free networks. This case mimics the turn-off of a whole group of genes, with some genes being hubs. A similar set-up is used in the simulation studies in (Danaher et al., 2014) and (Yuan et al., 2017).
3. **Star/hub graph:** Start with a scale-free network $G^{(1)}$. Then, identify a hub (or two, depending on the desired sparsity level) – a vertex with the biggest degree. Remove all edges, incident to that vertex, and obtain a graph $G^{(2)}$. The differential network G^{diff} is therefore a star graph. This case mimics an inhibition of a gene. The simulation studies of (Liu, 2017) and (Zhao and Shojaie, 2022) have similar set-ups, although with a higher number of less prominent hubs.

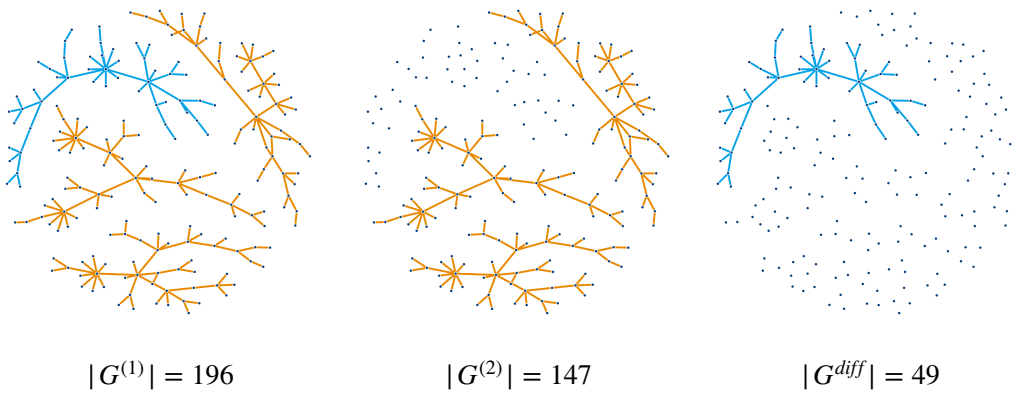
For all graph structures, there are several ways to vary the sparsity of $G^{(1)}$ and G^{diff} :

1. Fix $|G^{diff}|$ and vary the size of the **whole condition-specific** graph $|G^{(1)}|$;

Random differential graph



Scale-free differential graph



Star differential graph

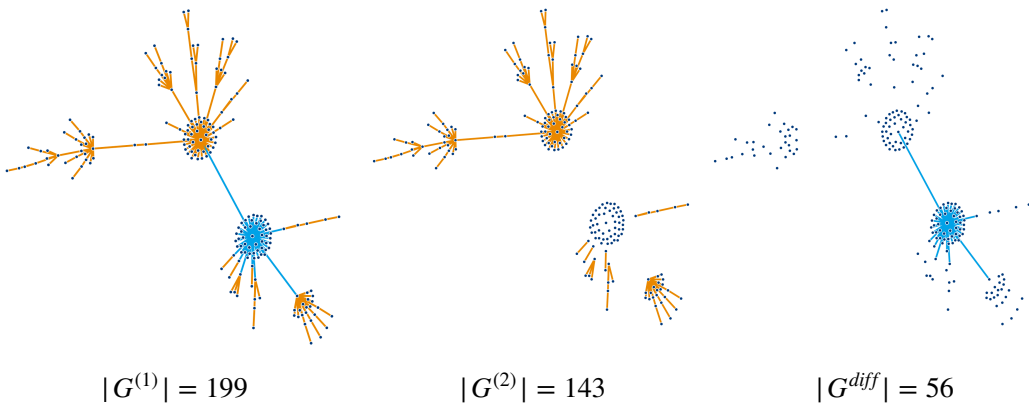


Figure 3: Graphs used in the simulation study for $|G^{(1)}| \approx 200$ and $|G^{diff}| \approx 50$ and 3 differential graph structures. Orange edges are common for $G^{(1)}$ and $G^{(2)}$; blue edges are differential, i.e. present only in $G^{(1)}$ or $G^{(2)}$.

2. Fix $|G^{(1)}|$ and vary the size of the **differential graph** $|G^{diff}|$;
3. Fix the proportion $|G^{(1)}|/|G^{diff}|$ and vary **both graphs'** sizes simultaneously.

In this work, we simulate all these three possibilities to assess the influence of a graphs' sparsity on the methods' performance.

All graphs have $p = 200$ vertices. The number of edges (size) of $G^{(1)}$ is determined by the number of edges added at each step of the Barabasi-Albert algorithm for scale-free graph generation, one or two. The size of G^{diff} and, consequently, $G^{(2)}$ is determined either by the rewiring procedure or the edge removal procedure. Since the graph generation steps are non-deterministic, they were re-run to achieve the best size consistency across different graph types and sparsity set-ups. The resulting graph sizes are given in Table 3. For simplicity, in the rest of the paper we will refer to the rounded-up graph sizes (50-200, 100-200, 50-400 and 100-400, respectively). We describe the graph generation procedure in detail in Appendix 4. See examples of generated graphs for the 50-200 edge setting in Figure 3 and all graphs in Figure (a) of Supplementary materials.

In the Discussion section, we will discuss properties of the pairs $(G^{(1)}, G^{(2)})$ and the corresponding differential graphs in connection with varying performance.

Table 3: Exact number of edges $(G^{(1)}, G^{(2)}, G^{diff})$ for different approximate sizes of $G^{(1)}$ and G^{diff} , and different graph types.

$ G^{(1)} $	Graph type	$ G^{diff} $	
		≈ 50	≈ 100
≈ 200	Random	(196, 196, 50)	(196, 196, 98)
	Scale-free	(196, 147, 49)	(196, 98, 98)
	Star	(199, 143, 56)	(199, 103, 96)
≈ 400	Random	(388, 388, 50)	(388, 388, 100)
	Scale-free	(388, 333, 55)	(388, 291, 97)
	Star	(397, 342, 55)	(397, 292, 106)

3.1.2 Data generation

For all graphs, we use the same data generating procedure. To construct precision matrices $\mathbf{\Omega}^{(1)}$ and $\mathbf{\Omega}^{(2)}$, we start with the graphs' adjacency matrices. We keep zeroes and replace non-zero entries, corresponding to network edges, with values sampled randomly from the uniform distribution with support on $[-0.9, -0.6] \cup [0.6, 0.9]$. Entries corresponding to the common edges in $\mathbf{\Omega}^{(1)}$ and $\mathbf{\Omega}^{(2)}$ are the same. We ensure symmetry by construction, i.e. we put the same value for (i, j) and (j, i) elements. To ensure positive definiteness (unless already achieved by construction), we make the matrices diagonally dominant by setting diagonal elements to $\Omega_{ii}^{(k)} = \sum_{j \neq i} |\Omega_{ij}| + 0.1$. We then invert each precision matrix and obtain $\mathbf{\Sigma}^{(1)}$ and $\mathbf{\Sigma}^{(2)}$. Finally, we sample $n_1 = n_2 = n$ independent identically distributed observations to obtain $\mathbf{X}^{(1)}$ and $\mathbf{X}^{(2)}$.

Two different sample sizes, $n_1 = n_2 = 100$ and $n_1 = n_2 = 400$, were chosen to reflect situations with $n < p$ and $n > p$. For biological applications, e.g. molecular networks, sample size is typically limited and higher sample sizes are not realistic for most studies. However, since we are estimating a graph, the number of parameters to estimate is not p but $p(p-1)/2$, which is an additional challenge. Although it is known that the number of samples influences the performance, we aim to study the magnitude of its impact.

For each pair $(G^{(1)}, G^{(2)})$, we generate 50 datasets and report all performance results as an average over the 50 sets.

3.1.3 Performance evaluation

For each method we vary either the regularization parameter λ (or λ_1 and λ_2) or the FDR level α to vary the size of \hat{E}^{diff} , from almost complete to almost empty. For each value of the parameter, we compare the estimated differential graph with the true differential graph and calculate the number of true and false positives as

$$TP = |\{(i, j) : (i, j) \in E^{diff} \cap \hat{E}^{diff}\}|,$$

$$FP = |\{(i, j) : (i, j) \in (E^{diff})^c \cap (i, j) \in \hat{E}^{diff}\}|.$$

For each method and each parameter value, we use TP and FP to calculate empirical power (how large proportion of the true edges a method was able to identify) and empirical false discovery rate (proportion of false edges among all identified) as

$$power = TP/|E^{diff}|,$$

$$FDR = FP/\max(1, FP + TP).$$

Considering these metrics across a range of tuning or regularization parameters for each method, we obtain a curve – see Figure 4.

Values of the parameters used in the simulation study are reported in Appendix 4. Simulation study code is available at github.com/annaplaksienko/Diff_networks_review_simulation.

3.2 Results

In Figure 4, we present the obtained results in terms of power versus false discovery rate for various methods (different colours), sparsity settings (sets of four facets in each panel of the figure), sample sizes (left and right set of facets in each panel) and differential graph structures (panels (a), (b) and (c)). We observe several challenges here.

For most settings, all methods exhibit the same trends depending on the graph structure and sparsity. Comparing various differential graph structures (see panels (a), (b) and (c) of Figure 4), we observe that the performance is the best for the random differential graph. It then gets worse for the scale-free graph and finally, the power is very low for almost all methods in all settings for the star differential graph. In other words, the more "structure" there is in a differential graph, the worse the performance becomes. Moreover, we notice that in most cases, the size of G^{diff} has little effect on performance while an increase in size of $G^{(1)}$ from ≈ 200 to ≈ 400 edges influences performance dramatically (compare sets of four facets in each panel and notice how performance drops from the first to the second row). For the random differential graph, the main drop in performance seems to happen when both the size of $G^{(1)}$ and the size of G^{diff} are increased simultaneously. We address these points in the Discussion section.

Regardless of the differential graph structure or size, we observe a significant deterioration of performance with a decrease from 400 to 100 samples (compare left and right set of facets in each panel of Figure 4), as expected. Although sample size thresholds depending on problem dimension p and the number of non-zero elements (edges) exist for many sparse application problems (see (Wainwright, 2009) for lasso, for example), to our knowledge, there are no results specific to differential graph estimation yet.

The best performance overall across all settings is demonstrated by direct estimation with lasso penalized D-trace loss (green "Dtrace" line in plots). It relies on direct estimation and focuses on the most distinct

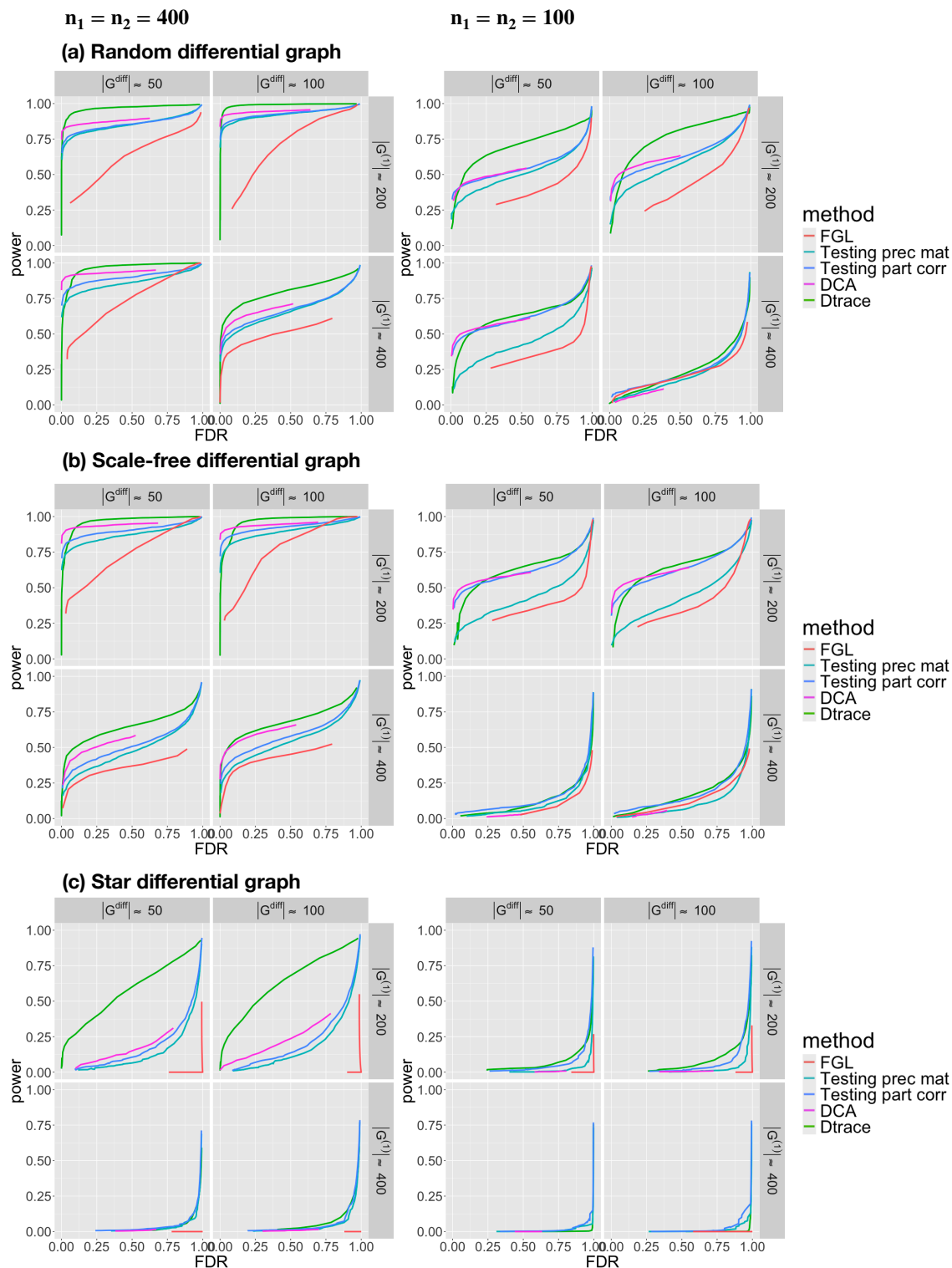


Figure 4: Estimated power vs FDR for the five considered methods in various sparsity and differential graph structure settings, with varying sample size. Results are averaged over 50 realizations of data.

minimization problem. In most settings the difference in performance may not be large (although still noticeable), but in the 50-200 and 100-200 star differential graph setting it demonstrates a clear advantage compared to other methods.

All testing methods demonstrate very similar performance, with DCA (pink line) providing a slightly higher power. For very low FDR, all three methods often demonstrate better power than the above-mentioned Dtrace method.

The joint estimation method FGL demonstrates the worst performance. In particular, for the star differential graph, this method has virtually no power at all.

4 Discussion

We have investigated the performance of five different methods for differential network estimation under varying graph structure, sparsity and sample size. Overall, we find lasso penalized D-trace loss to perform the best. However, given our focus on structure learning, one clear drawback of this method is the lack of formal error control. This is an area for future research.

The worst performance was shown by the joint estimation method FGL. This is not so surprising, as the method is constructed for an entirely different purpose. The method has two tuning parameters. One of them is driving sparsity, while the other one is targeted towards the degree of similarity between the precision matrices, not differences. Moreover, the necessity to tune two parameters is in itself a drawback compared to the other methods. This problem may be solved as suggested in (Lingjærde and Richardson, 2023) with a combination of stability selection and an extended Bayesian information criterion.

Regarding the error control, methods for testing the equality of entries of precision matrices or partial correlations both controlled FDR at the nominal level α , with the exception of star graph settings, where methods were much less stable and occasionally empirical FDR exceeded α . DCA was more conservative, with empirical FDR lower than the target level in most cases. We note that DCA provides a collection of raw p -values that we corrected for multiplicity with the Benjamini Hochberg procedure. It is likely that a more careful consideration of the specific multiple testing issue arising here could lead to a more efficient, less conservative solution. See Figure (b) in the Supplementary materials for more details.

We found that, overall, performance was primarily related to graph structure. We would like to investigate this a bit further.

We expect that performance of methods for learning differential networks depends on various properties of underlying graphs and probability distributions. To gain further insight, various measures of these properties can be employed. We considered two measures: one that corresponds to a global distance between distributions $\mathcal{N}(0, \Sigma^{(1)})$ and $\mathcal{N}(0, \Sigma^{(2)})$, and one that summarises the local structure of a differential graph.

We evaluate the global distance between distributions using symmetrized Kullback-Leibler divergence $KL_{12} + KL_{21}$, where for two centered Gaussian distributions $\mathcal{N}(0, \Sigma^{(i)})$, $i = 1, 2$, the Kullback-Leibler divergence KL_{ij} , $i, j = 1, 2$, is defined as

$$KL_{ij} = \frac{1}{2} \left\{ \text{tr} \left(\left[\Sigma^{(j)} \right]^{-1} \Sigma^{(i)} \right) - \log \frac{\det \Sigma^{(i)}}{\det \Sigma^{(j)}} - p \right\}.$$

To quantify local differences, we use the highest vertex degree of a differential graph divided by the total number of vertices p . Note that normalization by p is not necessary in the presented simulation as all graphs have the same size, $p = 200$, but we use it for possible comparison with other studies.

And finally, to summarize performance curves with a scalar, we compute the area under the curve (for power vs FDR) for $n = 400$ samples and average it over all five methods. We relate this performance indicator to the symmetrized Kullback-Leibler divergence and to the highest vertex degree. The resulting plots are shown in Figure 5.

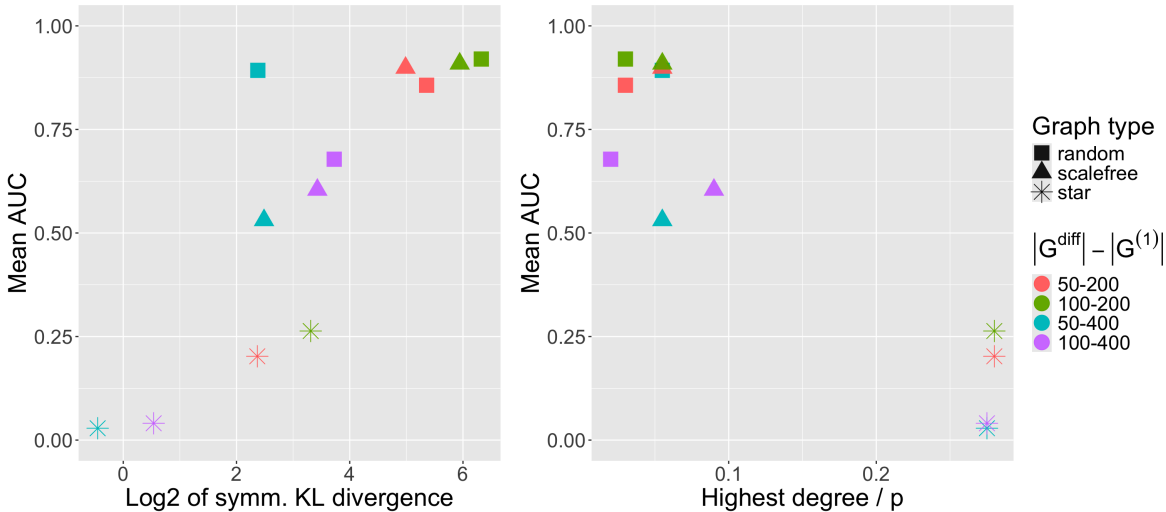


Figure 5: Averaged mean area under the power vs. FDR curve as a function of the symmetrized Kullback-Leibler divergence (left panel) and the highest vertex degree of a differential graph (right panel).

The left panel of Figure 5 demonstrates that methods on average perform better for sufficiently distant distributions (e.g. the cases of random and scale-free graphs in 50-200 and 100-200 edges settings). In other words, the larger the global differences are, the easier it is to estimate them correctly. One interesting observation is that performance can vary considerably for a given distance (e.g. three points having a similar value of log2 of symmetric KL divergence ≈ 2.4). This, however, may be at least partially explained by the highest degree (right panel). If the highest degree is sufficiently low, performance is good despite limited global difference.

We notice that for the star differential graph, the distance between distributions is low and the normalized highest degree is high in all settings. It is well known that hub structures are harder to estimate, as most methods assume uniform distribution of edges, without any specific structure (see discussion in (Tan et al., 2014), for example). Therefore, more information is required for a successful estimation in these situations. Indeed, for one of the methods (testing for equality of precision matrix entries, since it is one of the fastest) we have evaluated the performance for higher samples sizes, $n_1 = n_2 = 1000, 2000$, and discovered a considerable improvement (see Figure (c) in the Supplementary materials). We assume this observation may be applicable to other methods as well. Although increased sample size may be unachievable in many situations, aiming for as many samples as possible is advisable.

In the absence of larger samples, another option for improving performance in situations with hubs is to incorporate prior hub knowledge in the analysis. Such knowledge is often available, e.g. in the context of certain types of molecular networks. For instance, the joint estimation method *jewel* (Angelini et al., 2022)

is using user-provided class-specific degrees to construct edge weights which are then incorporated into the penalty terms for the method.

Methods for learning individual networks with hub structure do also exist, see e.g. the hub graphical lasso (Tan et al., 2014) or the hub weighted graphical lasso (McGillivray et al., 2020). Methods such as the perturbed node graphical lasso (Mohan et al., 2014) estimates two individual networks jointly taking into account potential hub differences. A possible direction of future work could be to extend such methods to the differential network situation, e.g. by using their estimands as an input for the testing-based methods described in the current paper.

In the current work we focused on networks with hubs since they often find application in modeling of biological networks. However, we expect that the observed challenges for the existing statistical methods carry over to more general community structures.

Finally, related to sample size, it would be desirable to obtain theoretical results on the necessary sample size n in relation to the differential graph order p and its maximum degree, as done, for example, for Ising models (Ravikumar et al., 2010).

Appendix A: Real data settings

Here, we provide the parameters used to estimate a 10-edge network in the real data example.

- For fused graphical lasso (FGL) (Danaher et al., 2014), implemented in the package `JGL`, we set $\lambda_1 = 0.1$ (as we empirically found this value to show good performance in our simulation studies), $\lambda_2 = 0.392$ and select a differential edge if $|\hat{\Omega}_{ij}^{(1)} - \hat{\Omega}_{ij}^{(2)}| > 10^{-3}$ (as the authors do in the code accompanying their manuscript);
- For the method testing for equality of partial correlations (Liu, 2017), implemented in the package `DiffNetFDR` (Zhang et al., 2019), we set $\alpha = 0.025$;
- For the method testing for equality of entries of precision matrices, implemented in the package `DiffNetFDR` (Zhang et al., 2019), we set $\alpha = 0.06$ (note that this result is the only one with 11 edges, as we were not able to obtain 10);
- For the differential connectivity analysis method (Zhao and Shojaie, 2022) implemented in the package `DCA`, we set $\alpha = 0.02$;
- For the direct estimation with lasso penalized D-trace loss (Yuan et al., 2017) (referred to as `Dtrace` for short in this manuscript), implemented in the package `DiffGraph` (Zhang et al., 2018), we set $\lambda = 0.555$.

Appendix B: Simulation study data generation

As described in the article, we have three differential graph structures: random, scale-free, and star. Let us first focus on the first two, random and scale-free, when $|G^{(1)}| \approx 200$. We start with the same graph $G^{(1)}$. We use `barabasi.game` from the `igraph` package to generate four disconnected scale-free networks, each with the power of preferential attachment (parameter `power`) equal to 1 and the number of edges added at each step of the generative algorithm equal to 1 (parameter `m`). The resulting graph $G^{(1)}$ has 196 edges.

Then, to obtain a scale-free differential network, we remove either one or two scale-free networks, resulting in graphs G^{diff} of sizes 50 or 98. To obtain a random differential network, we use a rewiring procedure that is performed with the `rewire(..., keeping_degseq())` function from the `igraph` package with a parameter `niter` set to 15 or 30 and re-run several times to obtain G^{diff} of sizes 49 and 98.

The procedure is the same when $G^{(1)} \approx 400$, but now each of the four disconnected scale-free networks has $m = 2$ edges added at each step of the generative procedure, resulting in a subgraph of ≈ 100 edges. To obtain a random differential network in the 50-400 and 100-400 settings, we use the same `rewire(..., keeping_degseq())` function with a parameter `niter` set to 30 or 60 and re-run several times until we achieve the desired differential network size. To obtain a scale-free differential network in the 100-400 setting, we remove one of the disconnected subnetworks of $G^{(1)}$. To obtain G^{diff} in the 50-400 setting, we construct a subgraph of that disconnected subnetwork in the following way: going from the vertex with the highest degree to the vertex with the lowest degree, we remove half of the incident edges of that vertex, controlling at each step that the number of connected components of G^{diff} is equal to 1 (except for isolated vertices). This is done to preserve the scale-free structure as much as possible.

Next, we will describe the generation of the star differential graph. To obtain the 50-200 and 100-200 settings, we first re-run the `barabasi.game` function with `m = 1` and `power = 1.7` until we obtain a graph that has two "hubs" (vertices with the highest degrees) of a similar size, 56 and 48. Then we remove all edges incident to one of them to obtain a 50-200 setting (the differential graph is a star graph) and all edges incident to both of them to achieve a 100-200 setting (the differential graph consists of two star graphs connected with one edge). To obtain the 50-400 and 100-400 settings, we re-run the `barabasi.game` function with `m = 2` and `power = 1.5` until we obtain a graph that has two "hubs" of similar size, 55 and 51. We then repeat the procedure described above.

Plots of all generated graphs can be found in Figure (a) of Supplementary materials. Code used to generate all graphs is freely available at github.com/annaplaksienko/Diff_networks_review_simulation

Appendix C: Simulation settings

Here we provide the parameters used to construct the power vs FDR curve in our simulation studies. We used the same set of parameters to produce the curves in all graph settings. We used default convergence parameters for all methods.

- For fused graphical lasso (FGL) (Danaher et al., 2014), implemented in the package `JGL`, we fix the "sparsity" tuning parameter $\lambda_1 = 0.1$ as we observed it provides good performance and we vary the "similarity" tuning parameter λ_2 from 0.01 to 0.5. We define an edge (i, j) as differential if $|\hat{\Omega}_{ij}^{(1)} - \hat{\Omega}_{ij}^{(2)}| > 10^{-3}$, following authors code, accompanying their paper;
- For the method testing for equality of partial correlations (Liu, 2017), implemented in the package `DiffNetFDR` (Zhang et al., 2019), we vary FDR level α from 0.001 to 0.995;
- For the method testing for equality of entries of precision matrices (Xia et al., 2015), implemented in the package `DiffNetFDR` (Zhang et al., 2019), we vary FDR level α from 0.001 to 0.995;
- For the differential connectivity analysis method (Zhao and Shojaie, 2022) with default GraceI test, implemented in the package `DCA`, we vary FDR level α from 0.0001 to 0.95;

- For the direct estimation with lasso penalized D-trace loss (Yuan et al., 2017) (referred to as Dtrace for short in this manuscript), implemented in the package `DiffGraph` (Zhang et al., 2018), we vary the tuning parameter λ from 0.1 to 0.7.

Data availability

The raw breast cancer data used in our motivating example is available at https://gdc.cancer.gov/about-data/publications/brca_2012 as `BRCA.exp.547.med.txt` (microarray gene expression) and `BRCA.547.PAM50.SigClust.Subtypes.txt` (cancer subtypes). The pre-processed dataset we used is a part of `DiffNetFDR` package (Zhang et al., 2019) as a `TCGA.BRCA` object.

Acknowledgments

This work is supported in part by the Norwegian Cancer Society, project number 216137.

References

- Angelini, C., De Canditiis, D., and Plaksienko, A. (2022). Jewel 2.0: An Improved Joint Estimation Method for Multiple Gaussian Graphical Models. *Mathematics*.
- Belilovsky, E., Varoquaux, G., and Blaschko, M. B. (2016). Testing for Differences in Gaussian Graphical Models: Applications to Brain Connectivity. In *Proceedings of Conference on Neural Information Processing Systems (NeurIPS)*.
- Danaher, P., Wang, P., and Witten, D. M. (2014). The joint graphical lasso for inverse covariance estimation across multiple classes. *Journal of the Royal Statistical Society, Series B*, 76(2):373–397.
- Giraud, C. (2015). *Introduction to High-Dimensional Statistics*. Chapman and Hall/CRC.
- Guo, J., Levina, E., Michailidis, G., and Zhu, J. (2011). Joint estimation of multiple graphical models. *Biometrika*, 98(1):1–15.
- He, H., Cao, S., Zhang, J. g., Shen, H., Wang, Y. P., and Deng, H. w. (2019). A Statistical Test for Differential Network Analysis Based on Inference of Gaussian Graphical Model. *Scientific Reports*, 9(1).
- Kanapathy Pillai, S. K., Tay, A., Nair, S., and Leong, C. O. (2012). Triple-negative breast cancer is associated with EGFR, CK5/6 and c-KIT expression in Malaysian women. *BMC Clinical Pathology*, 12.
- Kanehisa, M. and Goto, S. (2000). KEGG: Kyoto Encyclopedia of Genes and Genomes. *Nucleic Acids Research*, 28(1):27–30.
- Koboldt, D. C., Fulton, R. S., Schmidt, H., Kalicki-Veizer, J., and et al (2012). Comprehensive molecular portraits of human breast tumours. *Nature*, 490(7418):61–70.
- Lauritzen, S. L. (1996). *Graphical models*. Clarendon Press, Oxford.
- Lingjærde, C. and Richardson, S. (2023). StabJGL: a stability approach to sparsity and similarity selection in multiple-network reconstruction. *Bioinformatics Advances*, 3(1):vbad185.

- Liu, W. (2017). Structural similarity and difference testing on multiple sparse Gaussian graphical models. *Annals of Statistics*, 45(6):2680–2707.
- McGillivray, A., Khalili, A., and Stephens, D. A. (2020). Estimating sparse networks with hubs. *Journal of Multivariate Analysis*, 179.
- Meinshausen, N. and Bühlmann, P. (2006). High-dimensional graphs and variable selection with the Lasso. *Annals of Statistics*, 34(3):1436–1462.
- Mohan, K., London, P., Fazel, M., Witten, D., and Lee, S.-I. (2014). Node-Based Learning of Multiple Gaussian Graphical Models. *Journal of Machine Learning Research*, 15(1).
- Nalwoga, H., Arnes, J. B., Wabinga, H., and Aklsen, L. A. (2008). Expression of EGFR and c-kit is associated with the basal-like phenotype in breast carcinomas of African women. *APMIS*, 116(6):515–525.
- Ravikumar, P., Wainwright, M. J., and Lafferty, J. D. (2010). High-dimensional Ising model selection using l_1 -regularized logistic regression. *The Annals of Statistics*, 38(3):1287 – 1319.
- Shojaie, A. (2021). Differential network analysis: A statistical perspective. *Wiley Interdisciplinary Reviews: Computational Statistics*, 13(2).
- Tan, K. M., London, P., Mohan, K., Fazel, M., Witten, D., Lee, S.-I., and Tan, D. W. (2014). Learning graphical models with hubs. *Journal of Machine Learning Research*, 15:3297–3331.
- Wainwright, M. J. (2009). Sharp thresholds for high-dimensional and noisy sparsity recovery using l_1 -constrained quadratic programming (Lasso). *IEEE Transactions on Information Theory*, 55(5):2183–2202.
- Xia, Y., Cai, T., and Cai, T. T. (2015). Testing differential networks with applications to the detection of gene-gene interactions. *Biometrika*, 102(2):247–266.
- Yuan, H., Xi, R., Chen, C., and Deng, M. (2017). Differential network analysis via lasso penalized D-trace loss. *Biometrika*, 104(4):755–770.
- Zhang, X. F., Ou-Yang, L., Yang, S., Hu, X., and Yan, H. (2018). DiffGraph: An R package for identifying gene network rewiring using differential graphical models. *Bioinformatics*, 34(9):1571–1573.
- Zhang, X. F., Ou-Yang, L., Yang, S., Hu, X., and Yan, H. (2019). DiffNetFDR: Differential network analysis with false discovery rate control. *Bioinformatics*, 35(17):3184–3186.
- Zhang, Y., Liu, Y., Feng, L., and Wang, Z. (2023). Testing the differential network between two gaussian graphical models with false discovery rate control. *Journal of Statistical Computation and Simulation*.
- Zhao, H., Dai, P.-y., Yu, X.-j., He, J.-y., Zhao, C., and Yin, L.-h. (2023). Evaluation of graphical models for multi-group metabolomics data. *Briefings in Bioinformatics*.
- Zhao, S. and Shojaie, A. (2022). Network differential connectivity analysis. *Annals of Applied Statistics*, 16(4):2166–2182.
- Zhao, S. D., Cai, T. T., and Li, H. (2014). Direct estimation of differential networks. *Biometrika*, 101(2):253–268.

Zheng, X., Aragam, B., Ravikumar, P., and Xing, E. P. (2018). DAGs with NO TEARS: Continuous Optimization for Structure Learning. In *Proceedings of Conference on Neural Information Processing Systems (NeurIPS)*.